INTERNATIONAL JOURNAL OF CLIMATOLOGY
Int. J. Climatol. (2010)
Published online in Wiley Online Library
(wileyonlinelibrary.com) DOI: 10.1002/joc.2259

RMetS
Royal Meteorological Society

Interannual variation of Southern Hemisphere tropical cyclone activity and seasonal forecast of tropical cyclone number in the Australian region

Kin Sik Liu and Johnny C. L. Chan*

Guy Carpenter Asia-Pacific Climate Impact Centre, School of Energy and Environment, City University of Hong Kong, Tat Chee Ave., Kowloon, Hong Kong, China

ABSTRACT: This study examines the interannual variability of the tropical cyclone (TC) activity in the Southern Hemisphere (SH) during the period 1970–2008. An empirical orthogonal function analysis of the annual frequency of TC occurrence shows three leading modes of TC occurrence patterns. The first mode, which is related to the El Niño-Southern Oscillation (ENSO) phenomenon, shows an east-west oscillation between the anomalous TC activity over the South Pacific and the southern Indian Ocean. The second mode, characterised by an east-west dipole of anomalous TC activity over the southern Indian Ocean, is apparently related to both ENSO and the Indian Ocean dipole (IOD). The third is a basin-wide mode that represents the overall TC activity in the SH.

Within the SH, TC activity in the Australian region is found to be related to ENSO and IOD, with the relation being more prominent for the western Australian region. Basing on the ENSO- and IOD-related predictors such as Niño-4 SST anomaly, trade wind index, outgoing longwave radiation index and dipole-mode index, a statistical prediction scheme for the annual number of TCs in the entire Australian region (40 °S–0 °N, 90 °E–160 °E), the western Australian region (40 °S–0 °N, 90 °E–135 °E) and the eastern Australian region (40 °S–0 °N, 135 °E–160 °E) by 1 November is proposed. This scheme gives a 51, 39 and 37% skill improvement in root-mean-square error relative to climatology for the three regions respectively. Copyright © 2010 Royal Meteorological Society

KEY WORDS Southern Hemisphere tropical cyclone activity; Australian tropical cyclone activity; seasonal tropical cyclone prediction

Received 21 December 2009; Revised 12 October 2010; Accepted 19 October 2010

1. Introduction

Many previous studies (e.g. Nicholls, 1979, 1984, 1985, and 1992) have investigated the relation between the El Niño-Southern Oscillation (ENSO) phenomenon and tropical cyclone (TC) activity in the Australian region. More recently, Broadbridge and Hanstrum (1998) examined TC activity in the western Australian region and found that its connection to ENSO is less significant than the entire Australian region. Ramsay *et al*. (2008) investigated the role of large-scale environment factors in the interannual variability of TC activity in the Australian region. Kuleshov *et al*. (2008) examined the connection of the ENSO to the TC activity in the Southern Hemisphere (SH) and showed the differences in TC cyclogenesis and occurrence in El Niño and La Niña years. In addition to the effect of ENSO, Grant and Walsh (2001) examined the relation between the interdecadal variability of TC formation in the northeastern Australian region and the Interdecadal Pacific Oscillation. Some previous studies have also developed seasonal forecasts of TC activity in the Australian region (e.g. Nicholls, 1979, 1992). McDonnell and Holbrook (2004) proposed a statistical model for the seasonal forecast of TC activity in the Australian/southwest Pacific Ocean based on the Southern Oscillation Index (SOI) and the saturated equivalent potential temperature gradient. Flay and Nott (2007) also developed a statistical model for the prediction of TC landfalls in Queensland using the SOI. More recently, Goebbert *et al*. (2010) proposed a prediction scheme for the northwest Australian TC frequency based on a set of NCEP-NCAR reanalysis fields (geopotential height, air temperature, and components of wind) which are highly correlated with TC frequency.

While many previous studies focused on the variation of TC activity in the Australian region, only a few have examined the variation of TC activity in the entire SH. This study represents an attempt to investigate the interannual variation of the overall TC activity in the SH using an empirical orthogonal function (EOF) analysis and the possible relationships of such variations with climatic oscillations. The data used in this study are described in Section 2. The major modes of the variation of TC activity in the SH are shown in Section 3. The interannual variation of TC activity in the Australian region is then examined in Section 4. The atmospheric

* Correspondence to: Johnny C. L. Chan, School of Energy and Environment, City University of Hong Kong, Tat Chee Ave., Kowloon, Hong Kong, China. E-mail: Johnny.Chan@cityu.edu.hk

Copyright © 2010 Royal Meteorological Society

patterns associated with these variations of TC activity are next investigated in Section 5. Basing on the results discussed in Sections 3 and 4, a prediction scheme is proposed in Section 6. The summary and discussion are then given in Sections 7 & 8.

2. Data and methodology

2.1. Data

2.1.1. Best track data

The IBTrACS dataset is obtained from the World Data Center for Meteorology (http://www.ncdc.noaa.gov/oa/ibtracs/index.php). The 6-hourly best-track positions of TCs in the SH occurring between 1970 and 2008 are extracted. The IBTrACS position and intensity are taken as the means of the positions and intensities from different centres/agencies, respectively (Kruk *et al*., 2010). Only those positions at which a TC has the mean intensity with at least tropical depression strength are used to define the pattern of frequency of TC occurrence and the annual number of TCs occurring in the specified areas.

2.1.2. Atmospheric and oceanic indices and data

Potential predictors include ENSO indices, trade wind index, and outgoing long-wave radiation (OLR) index extracted from the website of U.S. Climate Prediction Center (http://www.cpc.noaa.gov/data/indices/). The dipole mode index (DMI), defined as the difference in SST anomaly between the tropical western (60 °E–80 °E, 10 °S–10 °N) and southeastern (90 °E–110 °E, 10 °S–0°) Indian Ocean, and used as a measure of the Indian Ocean Dipole (IOD) event (Saji and Yamagata, 2003), is obtained from the Frontier Research Center for Global Change (http://www.jamstec.go.jp/frcgc/research/d1/iod/).

Monthly 850-hPa zonal and meridional winds are obtained from the NCEP-NCAR reanalysis dataset. The horizontal resolution of the dataset is 2.5° latitude × 2.5° longitude.

2.2. Frequency of TC occurrence

The spatial distribution of TC activity in a year is represented by the annual frequency of TC occurrence. The 6-hourly positions of the TCs occurring between 1970 and 2008 are extracted from the best-track dataset first. The region 40 °S–0 °N, 30 °E–120 °W is divided into 5° latitude × 5° longitude grid boxes. The annual number of TCs passing through each box is then calculated. If a TC passes the same box more than once, it is counted only once. An EOF analysis is then applied to obtain the dominant modes of TC occurrence pattern.

3. Patterns of TC occurrence frequency

3.1. EOF analysis

3.1.1. Mode 1 (ENSO mode)

The first EOF of the TC frequency of occurrence explains ∼10.3% of the total variance and shows positive loadings over the South Pacific Ocean (Figure 1(a)). Positive maxima are found near 10 °S, 170 °E, and 10 °S, 170 °W, suggesting a higher frequency of TC genesis over these areas during the positive phase of this pattern. TCs formed over the latter area tend to move southeastward and have a longer lifespan, resulting in a large area

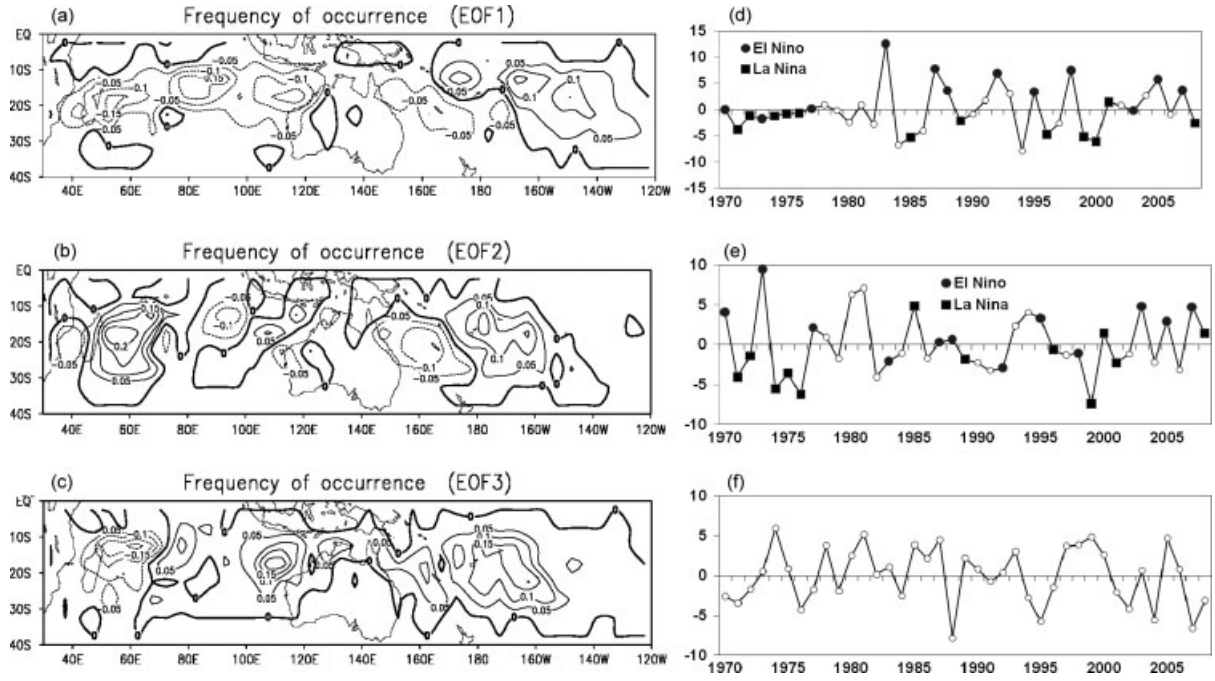

Figure 1. Loading patterns of anomalous TC frequency of occurrence for (a) EOF1, (b) EOF2, and (c) EOF3. Time series of PC1, and PC2 and PC3 are shown in (d)–(f). respectively.

Copyright © 2010 Royal Meteorological Society

of positive loadings east of 170 °W. A broad area of negative loadings is found west of 160 °E, extending from northeastern Australia to Madagascar. Therefore, this mode represents the east-west oscillation between the anomalous TC activity over the South Pacific and the southern Indian Ocean.

The time series of the EOF coefficients (PC1) suggests that this mode is only obvious after 1982 and generally shows positive values in El Niño and negative values in La Niña years, suggesting a possible connection of this mode to ENSO events (Figure 1(d)). As ENSO events usually peak in winter, the mean Niño-3.4 SST anomaly between December and February is used to represent the strength of ENSO. The PC1 coefficients are positively correlated with the Dec-Feb Niño-3.4 SST anomalies ($r = 0.73$). The eight years with the highest values of PC1 are all associated with El Niño events (1982/1983, 1986/1987, 1987/1988, 1991/1992, 1994/1995, 1997/1998, 2004/2005, and 2006/2007). The negative phase of this mode is mainly associated with La Niña events (1984/1985, 1995/1996, 1998/1999, and 1999/2000) except for the 1983/1984 and 1994/1995 season. Thus, this mode represents the interannual variation of the spatial distribution of TC activity in the SH associated with ENSO events.

Kuleshov *et al*. (2008) also examined the connection of ENSO to TC activity in the SH and showed that TC occurrence is higher over the southern Indian Ocean east of 80 °E but lower over the South Pacific Ocean east of 170 °E in La Niña in comparison to El Niño years, which is similar to the spatial pattern represented by this mode. Thus, the present results are consistent with the findings of Kuleshov *et al*. (2008).

3.1.2. Mode 2 (IOD/ENSO mode)

The second EOF explains ~8.0% of the total variance and its loading pattern is quite similar to that of EOF1 except for the east-west dipole over the southern Indian Ocean (Figure 1(b)). The distinct dipole feature of anomalous TC activity over the southern Indian Ocean suggests that this mode may be related to IOD events. Indeed, the coefficients of this EOF (PC2) are correlated with both the Sep-Nov DMI and Niño-3.4 SST anomalies, with correlation coefficients of 0.36 and 0.45, respectively. Therefore, this mode may be related to IOD as well as ENSO events.

In this study, a strong positive IOD event is defined if the Sep-Nov DMI is $>1\sigma$ (standard deviation) and a strong negative one with DMI $<-1\sigma$. During the period of 1970–2008, six strong positive IOD events are found in the Northern Hemisphere fall of 1972, 1982, 1987, 1994, 1997, and 2006, which are all associated with El Niño events. The high correlation ($r = 0.72$) between the Sep-Nov Niño-3.4 SST anomaly and DMI also suggests a possible connection between IOD and ENSO events. Of the six TC seasons following positive IOD events, three (1972/1973, 1994/1995, and 2006/2007) are dominated by this mode (Figure 1(e)). It is worth noting that El Niño events associated with these seasons are weaker except for the season 1972/1973. For the other three TC seasons associated with stronger El Niño events (1982/1983, 1987/1988, and 1997/1998), the positive phase of mode 1 is dominant. Hence, the positive phase of mode 2 may be prominent when the IOD is in its positive phase and the El Niño event is not strong.

The connection of negative IOD events to La Niña events appears to be weaker. Out of the seven stronger negative IOD events (1970, 1974, 1980, 1992, 1996, 1998, and 2005), only the 1970, 1974, and 1998 events are associated with La Niña events and these TC seasons are dominated by this mode (Figure 1(e)). For the other four TC seasons, this mode is insignificant.

It may be concluded that this mode is related to both IOD and ENSO events and may be significant in a TC season with co-occurring El Niño and positive IOD events or La Niña and negative IOD events.

3.1.3. Mode 3 (basin-wide mode)

The third EOF explains ~7.0% of the total variance and shows positive loadings over most of the areas, with larger amplitude between 170 °E and 160 °W, and between 100 °E and 120 °E (Figure 1(c)), and represents the overall TC activity in the SH. Indeed, the PC3 coefficients are highly correlated with the total annual number of TCs in the SH, with correlation coefficient of 0.60. The mean number of TCs in the SH during the positive phase and negative of this mode are 35.3 and 26.4, respectively, and the difference is statistically significant at the 99% confidence level.

3.2. Composite analysis

To test the significance of the three EOF modes, the separation between neighbouring eigenvalues with an estimate of the sampling error is compared (North *et al*., 1982). The eigenvalues associated with the first two EOFs are not well separated (Figure 2). A possible overlapping between EOF2 and EOF3 is also found. Nevertheless, it would still be of interest to investigate the effect of ENSO and IOD on the TC activity, which is accomplished through a composite analysis. The patterns of the anomalous frequency of TC occurrence in the ENSO years with and without IOD events are then compared.

For the El Niño years without the occurrence of a positive IOD event, namely 'pure' El Niño years, the composite frequency of TC occurrence shows positive anomalies over the South Pacific Ocean and negative anomalies over the southern Indian Ocean and the Australian region (Figure 3(a)), which is similar to the pattern of the positive phase of the first EOF (Figure 1(a)). For the El Niño years co-occurring with positive IOD events, the pattern over the southern Indian Ocean is different from that of pure El Niño years and is characterised by a dipole of anomalous TC activity, with enhanced activity west of 70 °E and suppressed activity east of 70 °E

Copyright © 2010 Royal Meteorological Society

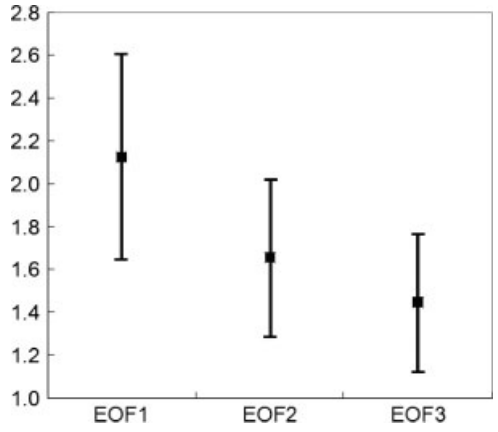

Figure 2. The eigenvalues corresponding to the first three EOFs. The error bars represent the standard error (one standard deviation error due to sampling).

(Figure 3(b)), which is very similar to the pattern of the positive phase of the second EOF.

The composite pattern for the pure La Niña years (without the occurrence of negative IOD event) is similar to the pattern associated with the negative phase of the first EOF (*cf* Figures 1(a) and 3(c)). Negative anomalies are generally found over the tropical South Pacific Ocean, and two areas of positive anomalies are found over the western southern Indian Ocean and the western Australian region, respectively. However, the pattern is quite different for the TC seasons with co-occurring La Niña and negative IOD events. A dipole is found over the southern Indian Ocean, with enhanced activity east of 70 °E and suppressed activity west of 70 °E (Figure 3(d)). In addition, a large area of enhanced TC activity is observed in the eastern Australian region. It appears that

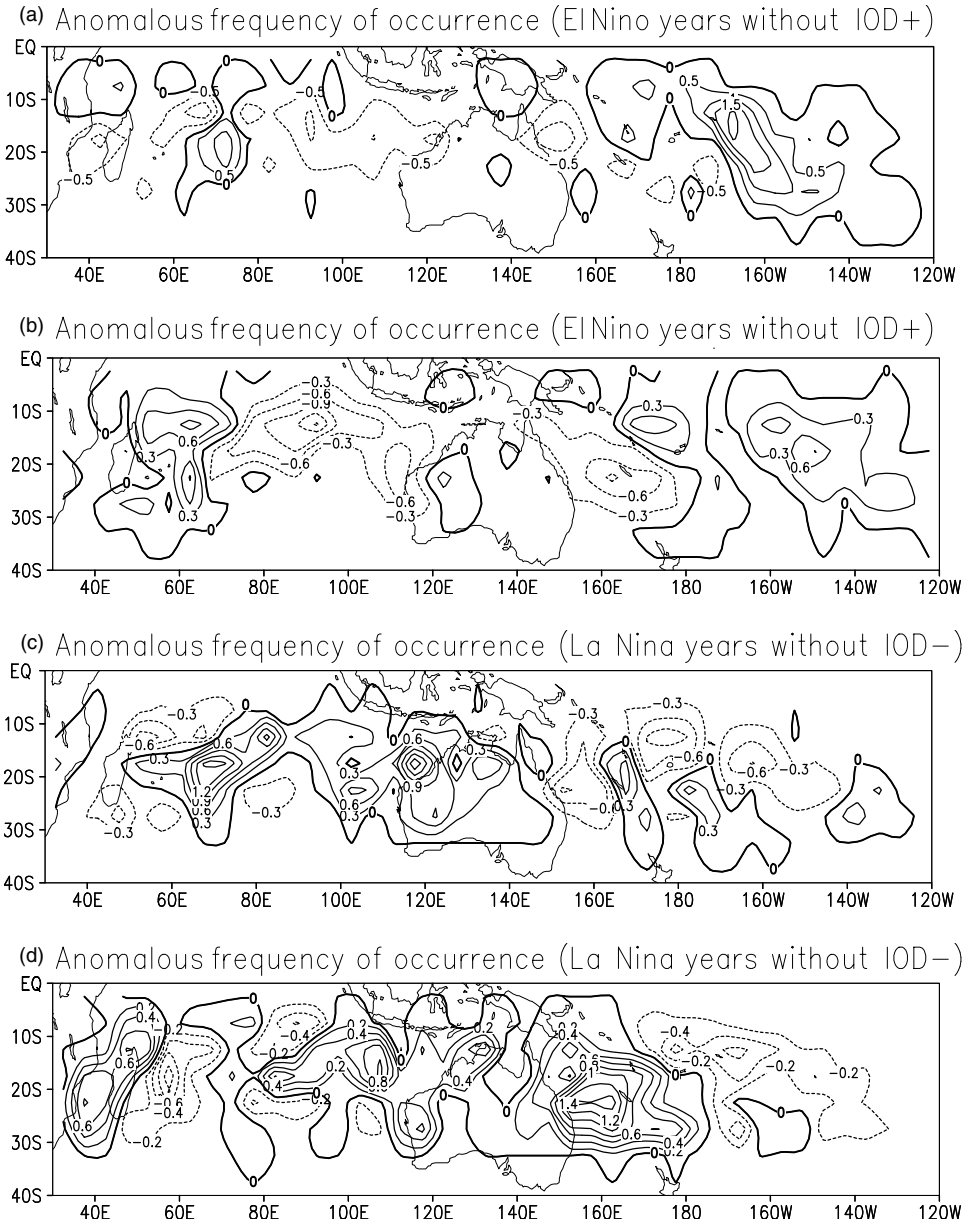

Figure 3. Anomalous frequency of TC occurrence in (a) pure El Niño years, (b) El Niño years co-occurring with positive IOD event, (c) pure La Niña years, and (d) La Niña years co-occurring with negative IOD event.

Copyright © 2010 Royal Meteorological Society

the regions of enhanced TC activity found in pure La Niña years shift eastward and cover the eastern southern Indian Ocean and the entire Australian region. These results suggest that TC activity in the eastern Australian region tends to be suppressed in pure La Niña years but enhanced in La Niña years co-occurring with negative IOD events. Thus, the combined effect of La Niña and negative IOD events appears to be mainly on the TC activity in the eastern Australian region and the influence on the western Australian region is relatively low.

The composite analysis has shown the interannual variability of the TC activity associated with ENSO, which may be represented by the first EOF of the frequency of TC occurrence. The composite ENSO/IOD patterns also suggest the modulation of IOD on the impact of El Niño event on the TC activity, which may also be reflected by the second EOF of the frequency of TC occurrence. Therefore, these results validate the findings obtained from the EOF analysis, despite the less-than-ideal separation between the first two EOFs.

4. Interannual variation of tropical cyclone activity in the Australian region

The variations of the spatial distribution of the TC activity in the SH have shown to be primarily represented by the three modes of TC occurrence frequency. Since the TC activity near land areas is more important from the point of view of the impact on human and economic activities, the focus of this section will be on the variation of the TC activity in the Australian region (40 °S–0 °N, 90 °E–160 °E), which is further divided into the western Australian region (90 °E–135 °E) and the eastern Australian region (135 °E–160 °E) in order to examine the spatial variation of the TC activity. A TC year in the Australian region spans from July to the following June and the peak TC season is from December to March. It should be noted that the sum of the TC numbers in the western and eastern Australian regions may not be equal to the TC number in the entire Australian region because some TCs may move across both the western and eastern Australian regions.

The results from the EOF analysis and composite analysis in Section 3 suggest that the interannual variation of the TC activity in the Australian region is related to ENSO and IOD events. The negative correlation between the mean Dec-Mar Niño-3.4 SST anomaly and the annual TC number in the entire Australian region ($r = -0.66$) suggests that TC activity tends to be below normal in a TC season associated with an El Niño event and above normal with a La Niña event, which is consistent with the results from previous studies (Nicholls, 1979, 1984, 1985, 1992; also shown in Figure 3). Of the 11 TC seasons associated with El Niño events, 8 are associated with below-normal TC number and a normal TC activity is found in the other 3 TC seasons (Table I). To examine the combined effect of IOD and ENSO events, the mean TC numbers in the seasons with and without positive IOD events are compared (Table I(a) and (b)). No significant difference is found in these TC numbers and therefore the modulation of IOD on the impact of El Niño event on the TC activity in this region may not be significant. For the TC seasons associated with La Niña events, TC activity is generally enhanced, with 7 of them having above-normal TC numbers (Table II). It is worth noting that the mean TC number in the seasons with negative IOD events is significantly higher than those without negative IOD event (*cf* Table II(a) and (b)), suggesting a possible combined effect of La Niña and negative IOD events on the TC activity. To conclude, the TC activity in the entire Australian region tends to be suppressed (enhanced) in an El Niño (La Niña) year. Indeed, the mean TC numbers for the TC seasons associated with El Niño and La Niña events are 9.6 and 16.7, respectively, and the difference is statistically significant at the 99% confidence level.

While it has been demonstrated that ENSO has a significant impact on the TC activity in the entire Australian region, it is useful to investigate its effect on the western and eastern Australian regions separately. The loading pattern of mode 1 shows a large negative magnitude in the western Australian region, suggesting that the ENSO effect is mainly on the western part of the

Table I. Annual number of tropical cyclones in the entire, western, and eastern Australian regions in (a) the El Niño years without positive IOD events, and (b) the El Niño years with positive IOD events. Bold and italic numbers indicate the above-normal and below-normal TC numbers, respectively. The normal numbers are 12–15, 9–10, and 5–6 for the entire, western, and eastern Australian regions, respectively.

(a) El Niño year without positive IOD event

TC season	Entire Australian region	Western Australian region	Eastern Australian region
1969/1970	*8*	*4*	*4*
1986/1987	*9*	*6*	5
1991/1992	*11*	*5*	6
2004/2005	12	10	*3*
Mean	10.0	6.3	4.5
S.D.	1.8	2.6	1.3

(b) El Niño year with positive IOD event

TC season	Entire Australian region	Western Australian region	Eastern Australian region
1972/1973	13	10	5
1976/1977	14	*6*	**8**
1982/1983	*7*	*5*	*2*
1987/1988	*6*	*4*	*2*
1994/1995	*8*	*6*	*3*
1997/1998	*11*	*6*	**7**
2006/2007	*7*	*5*	*2*
Mean	9.4	6.0	4.1
S.D.	3.2	1.9	2.5

Copyright © 2010 Royal Meteorological Society

Table II. Annual number of tropical cyclones in the entire, western, and eastern Australian regions in (a) the La Niña years without negative IOD events, and (b) the La Niña years with negative IOD events. Bold and italic numbers indicate the above-normal and below-normal TC numbers, respectively. The normal numbers are 12–15, 9–10, and 5–6 for the entire, western, and eastern Australian regions, respectively.

(a) La Niña year without negative IOD event

TC season	Entire Australian region	Western Australian region	Eastern Australian region
1988/1989	15	10	5
1995/1996	**16**	**13**	6
1999/2000	14	**12**	*3*
2000/2001	*11*	9	5
Mean	14.0	11.0	4.8
S.D.	2.2	1.8	1.3

(b) La Niña year with negative IOD event

TC season	Entire Australian region	Western Australian region	Eastern Australian region
1970/1971	14	9	**7**
1971/1972	**16**	*6*	**11**
1973/1974	**20**	**11**	**9**
1974/1975	**18**	**14**	5
1975/1976	**19**	**11**	**10**
1984/1985	**19**	**12**	**10**
1998/1999	**22**	**16**	6
Mean	18.3	11.3	8.3
S.D.	2.6	3.2	2.3

region (Figure 1(a)). The correlation coefficients between the mean Dec-Mar Niño-3.4 SST anomalies and the TC numbers in the western and eastern Australian regions are −0.62 and −0.34, respectively, suggesting that the ENSO event has a prominent effect on TC activity in the western Australian region but its influence is less significant for the eastern Australian region. The ENSO effect on TC activity in the western Australian region is similar to that of the entire Australian region. TC activity is generally suppressed (enhanced) in a TC season associated with an El Niño (a La Niña) event, with the mean TC numbers being 6.1 and 11.2, respectively, which is statistically significant at the 99% confidence level. However, no significant modulation of IOD on the impact of ENSO on the TC activity is observed in this region (Tables I and II).

The TC activity in the eastern Australian region is generally suppressed in a TC season associated with an El Niño event (Table I) but the influence is less obvious than the western Australian region, which is consistent with the smaller negative magnitude in this region found in the loading pattern of mode 1 (Figure 1(a)). For the pure La Niña years, the TC activity tends to be near normal (Table II(a)). However, enhanced TC activity is generally found in the La Niña years co-occurring with negative IOD events (Table II(b)). Therefore, the TC activity in this region shows a significant difference in the La Niña years with and without negative IOD events, which is consistent with the difference in the composite patterns of the anomalous frequency of TC occurrence between these two groups (Figure 3(c) and (d)).

These results demonstrate the possibility of developing a seasonal forecast of the TC number in the Australian region based on the ENSO-related indices and the precursor of ENSO event. For the sub-regions of the Australian region, a seasonal prediction for the western and eastern Australian regions is also possible but the predictability could be relatively low for the eastern Australian region. The results in this section provide the basis for developing seasonal forecasts of the annual number of TCs occurring in the entire, western, and eastern Australian regions, which will be presented in Section 6.

5. Atmospheric patterns associated with ENSO and IOD events

5.1. El Niño and positive IOD events

The composite 850-hPa wind pattern for the pure El Niño years shows westerly anomalies over the tropical South Pacific Ocean east of 150 °E (Figure 4(a)), resulting in negative relative vorticity anomalies in this region (Figure 5(a)). The atmospheric conditions are therefore favourable for TC genesis and development, which is consistent with the enhanced TC activity in this region (Figure 3(a)). Easterly anomalies are found over the tropical southern Indian Ocean (Figure 4(a)) and a broad area of positive relative vorticity anomalies extends from the western southern Indian Ocean to the eastern Australian region (Figure 5(a)). The decrease in negative cyclonic vorticity tends to suppress TC activity in this region, which partly explains the suppressed TC activity in both the eastern and western Australian regions.

The composite 850-hPa wind pattern for the El Niño years co-occurring with positive IOD events is similar to that for the pure El Niño years (Figure 4(b)). However, a slight difference in the distribution of relative vorticity anomalies is found over the southern Indian Ocean (*cf* Figure 5(a) and (b)). Instead of a broad band of positive relative vorticity anomalies, a dipole of relative vorticity anomalies, with negative values west of 70 °E and positive values east of 70 °E, is found, which is consistent with the dipole of anomalous TC activity in this region (Figure 3(b)).

5.2. La Niña and negative IOD events

For the pure La Niña years, easterly anomalies are found over the equatorial Pacific Ocean east of 130 °E, with the maximum amplitude between 150 °E and 180 °E (Figure 4(c)). As a result, positive relative vorticity anomalies are observed in this region, which is not favourable for TC genesis and development (Figure 5(c)). Over the southern Indian Ocean, westerly anomalies

Copyright © 2010 Royal Meteorological Society

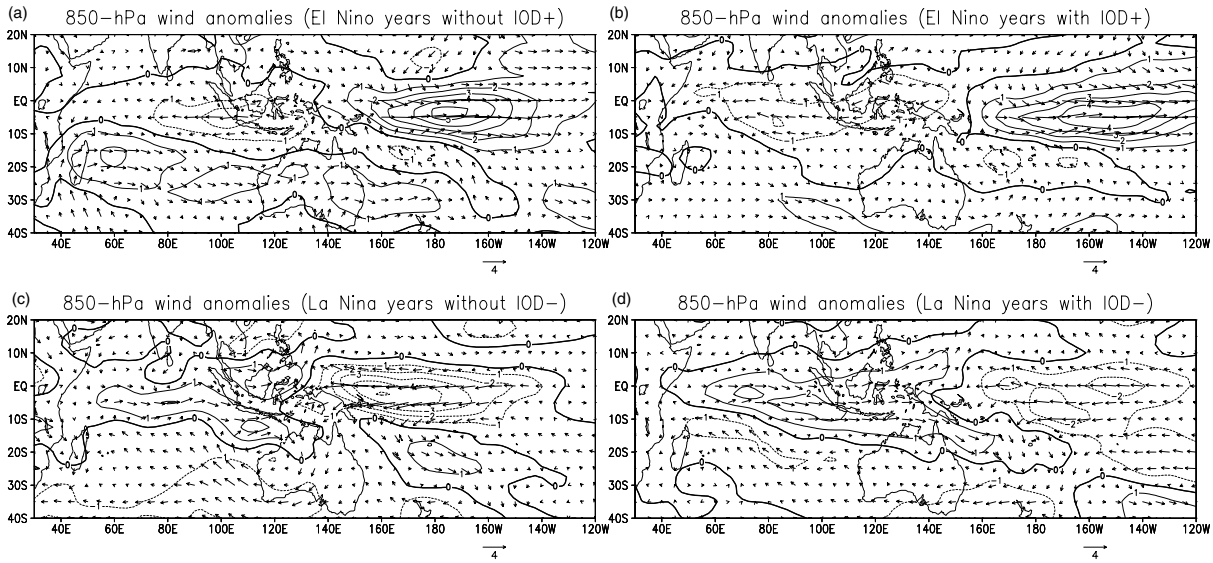

Figure 4. Composite of the 850-hPa wind anomalies in (a) pure El Niño years, (b) El Niño years co-occurring with positive IOD event, (c) pure La Niña years and (d) La Niña years co-occurring with negative IOD event. Contours indicate the zonal wind speed (contour interval: 1 m s^{-1}).

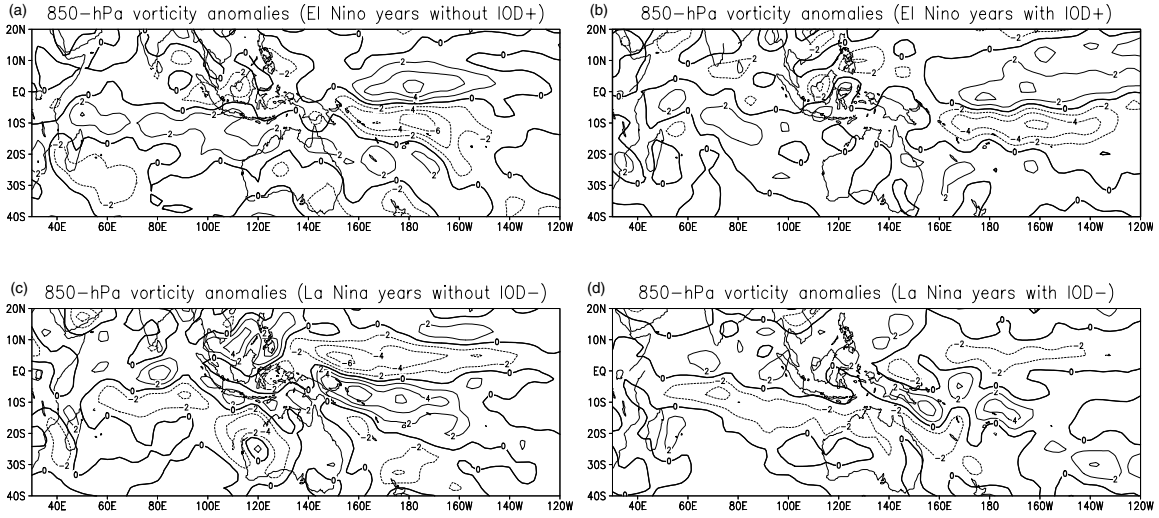

Figure 5. Composite of the 850-hPa relative vorticity anomalies in (a) pure El Niño years, (b) El Niño years co-occurring with positive IOD event, (c) pure La Niña years, and (d) La Niña years co-occurring with negative IOD event. (contour interval: 2×10^{-6} s^{-1}).

persist in the region between 0 °N and 10 °N and extend to the northwestern Australia (Figure 4(c)). TC activity is generally enhanced as a result of the favourable atmospheric conditions. Thus, this atmospheric pattern partly explains the suppressed TC activity in the eastern Australian region and the enhanced TC activity in the western Australian region.

The composite wind pattern is quite different for the La Niña years co-occurring with negative IOD events. The easterly anomalies over the tropical South Pacific Ocean are weaker and located more eastward (Figure 4(d)). The westerly anomalies over the southern equatorial Pacific Ocean are stronger and extend more eastward, covering the eastern Australian region and the ocean east of it. As a result, enhanced negative cyclonic relative vorticity is found in this region, which is consistent with the enhanced TC activity (Figure 5(d))

It can be seen that the atmospheric patterns associated with ENSO and IOD events is consistent with the corresponding patterns of anomalous TC frequency of occurrence and partly explain the interannual variability of the TC activity in the Australian region.

6. Seasonal forecast of tropical cyclone activity in the Australian region

The TC activity in the Australian region has been shown to have a significant interannual variation, which is primarily connected to the ENSO and IOD phenomena. These results suggest that the indices and precursors relating to these events may be good predictors for the seasonal forecast of the annual number of TCs occurring in the Australian region. As the main TC season usually begins in November, a statistical prediction scheme for

Copyright © 2010 Royal Meteorological Society

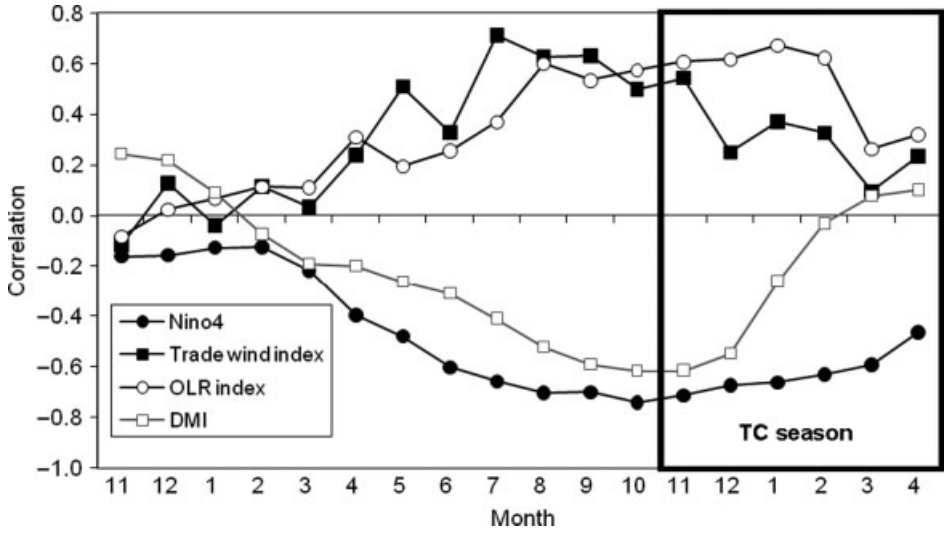

Figure 6. Correlations between the monthly values of the predictors from November of the previous year to April of the next year and the annual number of tropical cyclones in the entire Australian region. The thick box marks the TC season.

this TC number by 1 November is developed using the project-pursuit regression (PPR) technique (Friedman and Stueltzle, 1981) based on the information up to October. To identify the potential predictors, the monthly values of the indices relating to ENSO and IOD from November of the previous year to October of the current year are correlated with the annual TC number (example shown in Figure 6). Those indices with significant correlations with the TC number for at least three months are considered to be the possible predictors and will be further examined. The details of the identified predictors are discussed below.

6.1. Predictors

6.1.1. Nino-4 SST anomaly

The SST anomalies in the Niño-4 and Niño-3.4 regions are widely used as the indicators of ENSO events and therefore can be used as measures of the current state of ENSO and its trend. Since ENSO usually develops in the Northern Hemisphere spring or summer, their values in this period can be a precursor of a possible development of ENSO in the TC season (November-April) of the Australian region. The Niño-4 region index is chosen in the prediction scheme instead of the Niño-3.4 index because of its higher correlations with the TC numbers. The correlation becomes significant starting from April and has the higher values in the months of August–October (Figure 6). The mean Niño-4 SST anomaly averaged over the months August–October is highly correlated with the TC number in the Australian region ($r = -0.73$). In general, if this value is >0.5 (<-0.5), TC activity tends to be below normal (above normal). Similar results are obtained for the western and eastern Australian regions. Thus, these results suggest that the SST anomalies in the Niño-4 region can be a good indicator of the possible development of ENSO event and, thus, a possible predictor for the TC number. For a quantitative prediction of the TC number, the monthly values of the Niño-4 SST anomaly from November of the previous year to October of the current year are used.

6.2. Trade wind index over the west Pacific

The trade wind index over the west Pacific, defined as the mean 850-hPa zonal wind anomaly in the region (5 °S–5 °N, 135–180 °E), is a measure of the changes in zonal winds over the equatorial WNP. This index is closely related to ENSO as suggested by the high correlation with the Niño-3.4 SST anomalies and represents the changes in zonal winds associated with ENSO. The correlations between the monthly values of this index and the TC number in the entire Australian region are higher for the months between July and September (Figure 6). The mean Jul–Sep trade wind index is highly correlated with this TC number ($r = 0.68$), suggesting a close relation between the trade wind index and the TC activity in this region.

To examine this relationship further, the TC seasons are divided into two groups, one with trade wind index >1.0 (∼half of one standard deviation) and the other with trade wind index <-1.0. Out of the 8 TC seasons with a negative trade wind index, 7 are associated with the El Niño events and westerly anomalies are found over the equatorial WNP. Out of these TC seasons, 6 have below-normal TC activity and 2 have normal TC activity (Table III). For the 12 TC seasons with a positive trade wind index, 7 are associated with La Niña events and the others may be related to other climatic oscillations which are also connected to the changes in the atmospheric conditions and the TC activity in the Australian region. Out of these 12 TC seasons, 7 are associated with above-normal TC number and 4 with normal TC number (Table III). Indeed, the mean TC numbers in the TC seasons with negative and positive trade wind indices are 9.5 and 16.8, respectively, with the difference being statistically significant at the 99% confidence level. Similar relationships are found for the

Copyright © 2010 Royal Meteorological Society

Table III. Annual number of tropical cyclones in the entire, western, and eastern Australian regions in the seasons with positive and negative trade wind indices respectively. Bold and italic numbers indicate the above-normal and below-normal TC numbers, respectively.

Positive trade wind index					Negative trade wind index				
TC season	Trade wind index (Jul–Sep)	TC number			TC season	Trade wind index (Jul–Sep)	TC number		
		Entire	Western	Eastern			Entire	Western	Eastern
1998/1999	3.37	**22**	**16**	6	1982/1983	−4.90	*7*	*5*	*2*
1988/1989	3.03	15	10	5	1997/1998	−3.73	*11*	*6*	**7**
1999/2000	2.37	14	**12**	*3*	2002/2003	−2.67	12	9	5
1995/1996	2.37	**16**	**13**	6	1994/1995	−1.73	*8*	*6*	*3*
1989/1990	2.10	14	9	5	1987/1988	−1.47	*6*	*4*	*2*
2007/1908	1.93	14	**11**	*4*	1991/1992	−1.47	*11*	*5*	6
1996/1997	1.90	**18**	**12**	**7**	1980/1981	−1.37	14	**12**	*3*
2000/2001	1.47	*11*	9	5	2006/2007	−1.33	*7*	*5*	*2*
1983/1984	1.37	**21**	**15**	**8**					
1985/1986	1.23	**20**	**13**	**7**					
1981/1982	1.17	**18**	**14**	**8**					
1984/1985	1.07	**19**	**12**	**10**					
Mean		16.8	12.2	6.2	Mean		9.5	6.5	3.8
S. D.		3.3	2.2	2.0	S. D.		2.9	2.7	2.0

western and eastern Australian regions. Therefore, the trade wind index prior to the TC season can also be used as the predictor for the number of TCs occurring in these regions. This index may be better than the Niño-4 SST anomaly since it reflects the atmospheric conditions associated with ENSO as well as other climatic oscillations.

6.3. Outgoing long-wave radiation (OLR)

Outgoing long-wave radiation (OLR) index near the equator (160 °E–160 °W) represents the amount of convective activity near the equatorial WNP and central Pacific. The basis of the seasonal forecast of the annual TC numbers using the OLR index is similar to that of the trade wind index. This index has a close relationship with ENSO and usually shows negative (positive) value during the development of an El Niño (La Niña) event, representing the enhanced (suppressed) convective activity in this region. The mean Aug–Oct OLR index is correlated with the TC numbers in the entire Australian and the western Australian regions, with the correlation coefficients of 0.60 and 0.63, respectively. In general, if this value is >6.0 (half of its standard deviation), a development of a La Niña event is possible in the following TC season, so that the TC activity tends to be above normal. In contrast, the TC activity tends to be below normal if this value is <-6.0, indicating the possible development of an El Niño event and the below-normal TC activity in this region. The correlation between the OLR index and the TC number in the eastern Australian region is low and therefore this predictor is not used in the development of the seasonal forecast of the TC number in this region.

6.4. Dipole mode index (DMI)

As suggested in Sections 3 and 4, mode 2 of TC occurrence frequency is connected to the IOD event and the TC number in the Australian region. Therefore, DMI may be a possible predictor. Recall that the IOD event usually peaks in the months between September and November and a significant relation is found between the Sep–Nov DMI and the TC numbers (Section 4). A similar relation is also found for the Sep–Oct DMI (Figure 6), the correlation coefficient being 0.60. This relation allows the seasonal forecast of the TC numbers in the Australian regions.

6.5. Final prediction

Four potential predictors (Niño-4 index, trade wind index, OLR index and DMI) have been identified for the seasonal forecast of the annual numbers of TCs in the entire, western, and eastern Australian regions. It should be noted that the OLR index is not used for the eastern Australian region because of its low correlation with the TC number. The procedure used by Chan *et al.* (1998) in deriving the prediction equation is employed in this study. The regression equation is derived based on 28 years of data (1981–2008) for the trade wind index and OLR index and 39 years of data (1970–2008) for the other two predictors. For each predictor, the monthly values from November of the previous year to October of the current year (total 12 months) are considered. Five months are selected from these 12 months and the PPR technique is applied to derive the prediction equation. To ensure the prediction for each year is independent of the data for that year, the jackknife method is applied to each equation to make independent predictions, which are then correlated with the observed numbers. This step is repeated with different combinations of the five

Copyright © 2010 Royal Meteorological Society

Table IV. The predictors used in the scheme and the five selected months of each predictor used in the prediction equation for the entire, western, and eastern Australian regions. The corresponding linear correlation coefficients are also included. The months with superscripts (−1) and (0) indicate the months in the previous and current years, respectively.

Predictor	Selected months and corresponding linear correlation coefficient					
	Entire Australian region		Western Australian region		Eastern Australian region	
Niño4-SST anomaly	Nov^{-1}	0.00	Nov^{-1}	−0.04	Dec^{-1}	−0.24
	Jan^{0}	0.09	Dec^{-1}	−0.03	Jan^{0}	−0.18
	Feb^{0}	0.06	Mar^{0}	−0.12	May^{0}	−0.41
	Aug^{0}	−0.62	May^{0}	−0.37	Aug^{0}	−0.57
	Oct^{0}	−0.65	Oct^{0}	−0.59	Sep^{0}	−0.57
Trade wind index	Nov^{-1}	−0.12	Feb^{0}	0.11	Nov^{-1}	−0.29
	Jan^{0}	−0.04	May^{0}	0.52	Jan^{0}	−0.18
	Jul^{0}	0.71	Jun^{0}	0.35	Feb^{0}	0.16
	Aug^{0}	0.63	Jul^{0}	0.69	Jul^{0}	0.44
	Sep^{0}	0.63	Aug^{0}	0.63	Sep^{0}	0.24
OLR index	Dec^{-1}	0.02	Nov^{-1}	−0.05	–	–
	Mar^{0}	0.11	Mar^{0}	0.16	–	–
	Apr^{0}	0.31	Apr^{0}	0.36	–	–
	Jun^{0}	0.26	Jun^{0}	0.29	–	–
	Oct^{0}	0.57	Oct^{0}	0.62	–	–
DMI	Dec^{-1}	0.22	Jan^{0}	0.15	Feb^{0}	−0.15
	Mar^{0}	0.08	May^{0}	−0.21	Mar^{0}	−0.16
	Jun^{0}	−0.31	Jun^{0}	−0.24	May^{0}	−0.22
	Sep^{0}	−0.59	Sep^{0}	−0.46	Sep^{0}	−0.45
	Oct^{0}	−0.62	Oct^{0}	−0.49	Oct^{0}	−0.43

months and the equation with the highest correlation is retained, and the five months used in this equation are then considered to be mostly correlated with the TC number. These procedures are repeated for each of the predictors. The final prediction is then a linear, weighted combination of these forecasts, with the weights being the absolute value of the correlation coefficients estimated through the jackknife technique.

The five selected months used in the prediction equation and the corresponding linear correlation coefficients with the TC number of each predictor are shown in Table IV. While some monthly values appear to have a low linear correlation with the TC number, skill is added when they are combined with other months since non-linear relationships may exist and the PPR technique is capable of identifying such relationships by projecting the predictors onto different subspaces (Chan *et al*., 1998). It can be seen that the monthly value in the current September or October is selected in the derivation of the equation for all predictors, which might be expected because this value provides the latest information about the current status of the ENSO and IOD phenomena and, hence, the possible effect on TC activity. For the three ENSO-related predictors, the months in Northern Hemisphere spring or summer are also included. For the DMI predictor, the main contribution is from the values in September and October of the current year, the period when the IOD event usually attains its peak strength.

The performance of the prediction scheme is summarised in Table V. The correlation coefficients of the prediction by individual predictors range from 0.56 to 0.82, with the correlations being higher for the ENSO predictors, which might be expected because ENSO tends to be the major factor affecting TC activity in the Australian region. The correlation coefficients of the final prediction scheme, a weighted average of the forecasts from individual predictor, increase to 0.89, 0.80, and 0.79 for the entire, western, and eastern Australian regions, respectively. For the entire Australian region, the mean absolute error and root-mean-square error (RMSE) are 1.64 and 2.00, respectively. The performance of the scheme can also be seen from the scatterplot of the hindcasted *versus* observed values (Figure 7). A prediction can be considered to be correct if it falls within the dashed lines, which are parallel to the 45° line and constructed using the ±1 standard error from the prediction scheme. Out of the 39 predictions, 25 (∼64%) fall within this region for the entire Australian region, 29 (∼74%) for the western Australian region, and 29 (∼74%) for the eastern Australian region.

The scheme can also be evaluated based on the forecast skill S with respect to climatology (Wilks, 1995) which is defined as $S = \left(1 - \frac{\mathrm{RMSE}_{\mathrm{Scheme}}}{\mathrm{RMSE}_{\mathrm{Climatology}}}\right) \times 100\%$, where $\mathrm{RMSE}_{\mathrm{Scheme}}$ and $\mathrm{RMSE}_{\mathrm{Climatology}}$ are the root-mean-square errors of the forecasts based on the scheme and climatology, respectively. The value of S is found to be ∼51, 39 and 37% for the entire, western, and eastern Australian regions, respectively, which means that the scheme has a significant skill over climatology.

Copyright © 2010 Royal Meteorological Society

Table V. Performance of the prediction scheme.

Prediction by individual predictor			
Predictor	Correlation coefficient		
	Entire Australian region	Western Australian region	Eastern Australian region
Niño4-SST anomaly	0.82	0.56	0.61
Trade wind index	0.81	0.72	0.67
OLR index	0.77	0.74	–
DMI	0.67	0.56	0.65

Final prediction scheme			
	Entire Australian region	Western Australian region	Eastern Australian region
Correlation coefficient	0.89	0.80	0.79
Absolute error	1.64	1.70	1.06
Root mean square error	2.00	2.01	1.38
Forecast skill with respect to climatology (%)	51	39	37

7. Discussion

This study investigates the interannual variability of the TC activity in the SH based on the best-track data for the years 1970–2008 from the IBTrACS dataset. The spatial distribution of TC activity in a year is represented by the annual frequency of TC occurrence and an empirical orthogonal function analysis is applied to obtain the three leading modes of TC occurrence patterns. The first mode shows the east-west oscillation between the anomalous TC activity over the South Pacific and the southern Indian Ocean and is primarily connected to ENSO. In general, in a TC season associated with an El Niño (a La Niña) event, the TC activity over the South Pacific is enhanced (suppressed) while a suppression (an enhancement) of TC activity is found over the southern Indian Ocean. The second mode is characterised by an east-west dipole of anomalous TC activity over the southern Indian Ocean and is related to ENSO and IOD. A westward (eastward) shift of the TC activity over the southern Indian Ocean is usually observed during the positive (negative) phase of this mode. The third is a basin-wide mode and represents the overall TC activity in the SH. The composite analysis validates the results obtained from the EOF analysis.

The TC activity in the Australian region is shown to be related to ENSO and IOD, with the relation being more prominent for the western Australian region. In general, TC activity in the Australian region tends to be below (above) normal in a TC season associated with an El Niño (La Niña) event. For the sub-regions of the Australian region, similar results are found for the western Australian region. However, a modulation of the negative IOD event on the impact of La Niña on TC activity is found in the eastern Australian region. TC activity in the eastern Australian region tends to be near normal if no negative IOD event but above normal if co-occurring with negative IOD event.

The interannual variability of TC activity in the entire Australian region associated with ENSO and IOD events is partly related to the low-level wind patterns. The changes in the distribution of the relative vorticity anomalies are primarily responsible for the changes in TC activity.

The association between the ENSO and IOD phenomena and TC activity in the Australian region suggests that the parameters relating to these events might be good predictors. Four ENSO- and IOD-related predictors, Niño-4 SST anomaly, trade wind index, outgoing long-wave radiation index, and DMI, are found to be highly correlated to the annual number of TCs in the entire, western and the eastern Australian regions. A statistical prediction scheme for these numbers by 1 November is developed based on the project-pursuit regression technique. This scheme gives a 51, 39, and 37% skill improvement in root-mean-square error relative to climatology for the three regions respectively, which means that the scheme has a significant skill over climatology.

8. Conclusions

It has been demonstrated that ENSO is the main factor responsible for the interannual variations of the TC activity in the SH and some ENSO-related parameters have been identified for the seasonal forecast of the TC activity in the Australian region. These results are consistent with previous studies, some of which also provided a physical reasoning for such a relationship (e.g. Ramsay *et al*., 2008). Changes in the large-scale circulation associated with ENSO are primarily responsible for the variations of TC activity. Some ENSO-related parameters such as the Southern Oscillation Index have been suggested as the predictors for the seasonal forecast of TC activity in the Australian region (Nicholls,

Copyright © 2010 Royal Meteorological Society

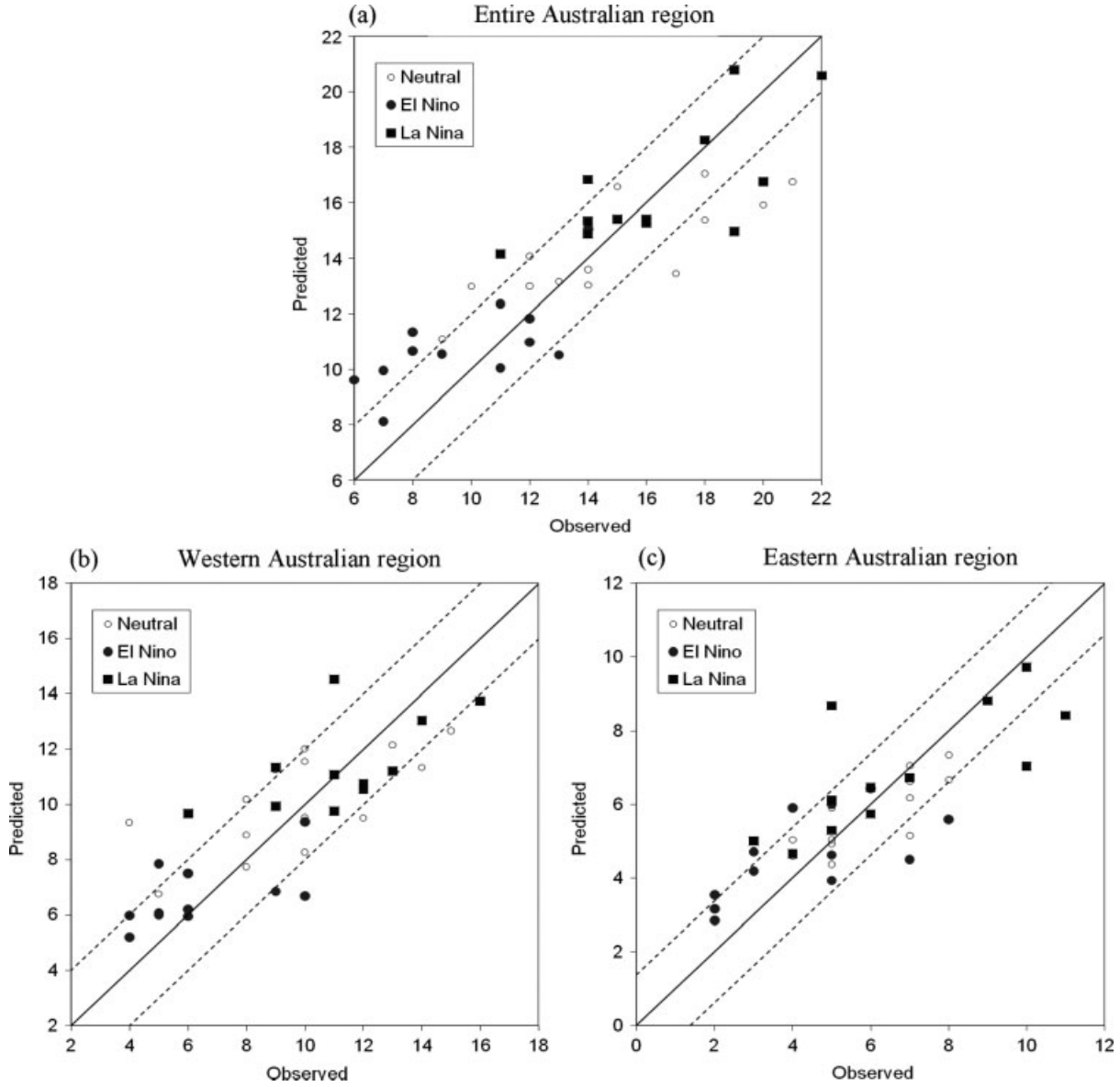

Figure 7. Scatterplot of the hindcasted *versus* observed values for the number of tropical cyclones in (a) the entire Australian region, (b) the western Australian region, and (c) the eastern Australian region. The solid line represents the prefect prediction and the two dashed lines are parallel to the solid line and deviate from it by a value that corresponds to the standard error of the predictions. Solid circles and squares indicate the TC seasons associated with the El Niño and La Niña events.

1979, 1992; McDonnell and Holbrook, 2004). Indeed, the Niño-4 SST anomaly has been used in the operational seasonal forecast by the Tropical Storm Risk group (http://www.tropicalstormrisk.com/). The present study suggests two additional predictors, the trade wind index and outgoing long-wave radiation index, which are shown to be capable of predicting the annual TC number in the Australian region and additional predictive skill is added when combining with the Niño-4 SST anomaly. These predictors might reflect the atmospheric conditions associated with ENSO as well as other climatic oscillations and therefore are the good predictors for the TC activity in the Australian region. Other than ENSO-related predictors, Goebbert *et al*. (2010) found a set of NCEP-NCAR reanalysis fields for the seasonal prediction of the northwest Australian (0°–35 °S, 105°–135 °E) TC frequency and obtained a fairly high skill over climatology. The predictors used in this study included the May–Jul 850-hPa geopotential heights over the south Indian Ocean, the Apr–Jun 700-hPa geopotential heights over Central North American, the May-Jul 850-hPa air temperatures over the central North Pacific and the Jun–Aug 925-hPa geopotential heights over the southern Atlantic Ocean and the eastern Pacific Ocean. It is of interest to see if similar predictors can be used for the seasonal prediction of TC numbers in the entire Australian region and the eastern Australian region.

While IOD may have an influence on the TC activity over the southern Indian Ocean, its physical connection to the variation of TC activity has not been addressed. Thus, a further study is required to investigate the oceanic and atmospheric conditions associated with IOD and the

Copyright © 2010 Royal Meteorological Society

subsequent influence on TC activity. The third mode of frequency of TC occurrence represents the overall TC activity in the SH and is important for not only the Australian region but also the other regions in the SH. However, no climatic oscillation connecting to this mode is identified and further investigation is therefore required to identify the related climatic oscillations.

References

Broadbridge LW, Hanstrum BN. 1998. The relationship between tropical cyclones near Western Australia and the Southern Oscillation Index. *Australian Meteorological Magazine* **47**: 183–189.

Chan JCL, Shi JE, Lam CM. 1998. Seasonal forecasting of tropical cyclone activity over the western North Pacific and the South China Sea. *Weather Forecasting* **13**: 997–1004.

Flay S, Nott J. 2007. Effect of ENSO on Queensland seasonal landfalling tropical cyclone activity. *International Journal of Climatology* **27**: 1327–1334.

Friedman JH, Stueltzle W. 1981. Projection pursuit regression. *Journal of the American Statistical Association* **76**: 817–823.

Goebbert KH, Leslie LM. 2010. Interannual variability of Northwest Australian tropical cyclones. *Journal of Climate* **23**: 4538–4555.

Grant AP, Walsh KJE. 2001. Interdecadal variability in north-east Australian tropical cyclone formation. *Atmospheric Science Letters* **2**: 9–17.

Kruk MC, Knapp KR, Levinson DH. 2010. A technique for combining global tropical cyclone best track data. *Journal of Atmospheric and Oceanic Technology* **27**: 680–692.

Kuleshov Y, Qi L, Fawcett R, Jones D. 2008. On tropical cyclone activity in the Southern Hemisphere: Trends and the ENSO connection. *Geophysical Research Letters* **35**: L14S08, DOI:10.1029/2007GL032983.

McDonnell KA, Holbrook NJ. 2004. A Poisson regression model approach to predicting tropical cyclogenesis in the Australian/southwest Pacific Ocean region using the SOI and saturated equivalent potential temperature gradient as predictors. *Geophysical Research Letters* **31**: L20110, DOI:10.1029/2004GL020843.

Nicholls N. 1979. A possible method for predicting seasonal tropical cyclone activity in the Australian region. *Monthly Weather Review* **107**: 1221–1224.

Nicholls. 1984. The southern oscillation, sea-surface temperature, and interannual fluctuations in Australian tropical cyclone activity. *Journal of Climatology* **4**: 661–670.

Nicholls. 1985. Predictability of interannual variations in Australian seasonal tropical cyclone, activity. *Monthly Weather Review* **113**: 1144–1149.

Nicholls. 1992. Recent performance of a method for forecasting tropical cyclone activity. *Australian Meteorological Magazine* **40**: 105–110.

North GR, Bell TJ, Cahalan RF, Moeng FJ. 1982. Sampling errors in the estimation of empirical orthogonal functions. *Monthly Weather Review* **110**: 699–706.

Ramsay HA, Leslie LM, Lamb PJ, Richman MB, Leplastrier M. 2008. Interannual variability of tropical cyclones in the Australian region: role of large-scale environment. *Journal of Climate* **21**: 1083–1103.

Saji NH, Yamagata T. 2003. Possible impacts of Indian Ocean Dipole Mode events on global climate. *Climate Research* **25**: 151–169.

Wilks DS. 1995. *Statistical Methods in the Atmospheric Sciences*. Academic Press Diego CA: pp. 467.

Copyright © 2010 Royal Meteorological Society